BUTTERWORTH HEINEMANN

Polymer Vol. 36 No. 5, pp. 1023–1033, 1995
Copyright © 1995 Elsevier Science Ltd
Printed in Great Britain. All rights reserved
0032-3861/95/$10.00+0.00

Molecular transport characteristics of Santoprene thermoplastic rubber in the presence of aliphatic alkanes over the temperature interval of 25 to 70°C

Tejraj M. Aminabhavi* and Hemant T. S. Phayde
Department of Chemistry, Karnatak University, Dharwad 580 003, India
(Received 6 May 1994; revised 7 July 1994)

Solvent transport into Santoprene thermoplastic rubber samples exposed to n-alkanes (C_5 to C_{16}), 2,2,4-trimethylpentane, cyclohexane and 1,2,3,4-tetrahydronaphthalene in the temperature interval 25–70°C has been studied. For all liquids, equilibrium penetrant uptake and degree of penetrant overshoot have been influenced by factors such as penetrant size, shape, polymer morphology and temperature. Sorption–desorption–resorption–redesorption experiments have been performed for some typical solvents at 25°C to determine the true sorption equilibrium and transport parameters. The values of the polymer–solvent interaction parameters have been used to calculate the molar mass between crosslinks of the network polymer. Kinetic rate constants and the activation parameters for the process of diffusion, permeation and sorption/desorption have been calculated. The transport coefficients and the activation parameters showed a dependence on the size of the penetrant molecules. The transport phenomenon was found to follow the Fickian-type mechanism.

(Keywords: Santoprene; diffusion; molecular transport)

INTRODUCTION

The molecular transport of organic solvents in rubbery polymers is a subject of both fundamental and technical importance[1–3]. It is fundamentally important because factors such as polymer morphology and molecular interactions that control the transport phenomenon are not well understood. Also, the existing transport theories, based on the macroscopic parameters, are difficult to interpret in terms of the interactions occurring between the polymer matrix materials and the diffusing molecules. It is technically important because the use of thermoplastic rubber products in applications such as barrier layers, cable coatings, etc., is extremely widespread[4]. Material failure in such applications might result in the loss of large amounts of capital investments. Polymer applications in areas such as landfill liners in hazardous waste treatment[5,6], reverse osmosis[7,8], pervaporation separation[2,9,10], etc., all require diverse characteristics of the film materials. Successful applications of polymers in these areas depend very much on their response to the presence of liquids.

Previous research efforts from our laboratory in this area have been directed towards the accumulation of extensive transport and sorption data of a variety of polymers in the presence of various organic liquids[11–18]. In these studies, liquid sorption or transport was found to be a function of structure of both the polymer and the diffusant molecule. The polymer chain orientation also seemed to modify the transport process. The present study extends these approaches toward molecular transport characteristics of a Santoprene thermoplastic rubber in the presence of aliphatic alkanes as probe molecules. Santoprene, i.e. miscible blends of ethylene–propylene random copolymer (EPM) and isotactic polypropylene, is a useful engineering polymer that combines the performance characteristics of vulcanized rubber with the processing ease of thermoplastics. The polymer is used in applications such as hose connectors, plugs, windshield spacers, vibration isolators, flexible cords, submersible cables, filter and pump seals, etc. However, acceptability of Santoprene for a specific application depends ultimately on its performance requirements and hence solvent exposure testing must be carried out before it is used.

Diffusion coefficients (D) and equilibrium sorption (M_∞) are the fundamental properties measured during solvent ingression studies. Some studies have indicated that the weight gain curves for polymers immersed in solvents show a decrease after reaching a maximum[19–21]. This phenomenon was attributed to diffusion of indigenous residual materials. The loss of low molecular weight residuals may be disastrous in some cases, e.g. the loss of residual to a packaged food. In several polymeric systems, the presence of solvents leads to a sudden overshoot effect which is followed by a decline to an equilibrium position. Such effects have been attributed to the relaxation processes within the polymer during solvent migration[20–22].

The objective of this study is to measure the sorption and transport characteristics of Santoprene as a function of temperature, solvent size, shape and polymer

* To whom correspondence should be addressed

morphology. A technique is proposed to assess the weight loss and thereby determine the sorption parameters. After sorption, polymer samples were desorbed to measure the amount of sorbed solvent and removal of any residuals. The desorbed samples were again exposed to solvent for resorption followed by redesorption. Thus, it appears that the sorption (S)–desorption (D)–resorption (RS)–redesorption (RD) test is an effective analytical probe for studying the molecular transport phenomenon in rubbery polymers. The sorption, diffusion and permeation coefficients of Santoprene–alkane systems have been estimated together with activation parameters to understand the behaviour of Santoprene in the presence of different solvents.

EXPERIMENTAL

Reagents and materials

Sheets of Santoprene rubber (sample designation 103-40) were obtained from Advanced Elastomer Systems (St. Louis, MO, USA) in dimensions of 26 cm × 26 cm with initial thicknesses ranging from 0.158 to 0.161 cm. Disc-shaped samples (diameter 1.97–1.99 cm) were cut from the large sheets by means of a sharp-edged carbon-tipped steel die. The test samples were dried in vacuum desiccators over anhydrous calcium chloride at room temperature for at least 24 h before experimentation. Some typical physical and mechanical property data of the samples are given in *Table 1*.

The reagent grade solvents used as penetrants were: n-pentane (BDH, UK), n-hexane and n-heptane (both S.D. Fine Chem. Ltd, Bombay, India), n-octane (Riedel, Germany), n-nonane, n-decane, n-dodecane, n-tetradecane and n-hexadecane (all from S.D. Fine Chem. Ltd), 2,2,4-trimethylpentane (BDH), cyclohexane (Ranbaxy Labs Ltd, Punjab, India) and 1,2,3,4-tetrahydronaphthalene (Riedel, Germany). Of these, 2,2,4-trimethylpentane, n-dodecane and 1,2,3,4-tetrahydronaphthalene were double distilled before use while the other solvents were used as supplied. Their measured physical properties such as densities and refractive indices at 25°C agreed well with the literature values[23]. Relevant data are given in *Table 2*.

Table 1 Typical mechanical and fluid resistance properties of Santoprene

Mechanical				Fluid resistivity[a]		
Properties	ASTM test method	Test temp. (°C)		Fluid	Test temp. (°C)	Volume swelling
Hardness (5 s Shore)	D2240	25	40D	Water	100	2
Specific gravity	D297	25	0.95	15% NaCl	23	0
Tensile strength (MPa)	D412	25	19.0	50% NaOH	23	0
Ultimate elongation (%)	D412	25	600	98% H_2SO_4	23	2
100% modulus (MPa)	D412	25	8.6	ASTM #1 oil	100	6
Tear strength (kN/m)	D624	25	64.6	ASTM #2 oil	100	17
		100	35.5	ASTM #3 oil	100	30
Tension set (%)	D412	25	48	Brake fluid	100	−9
Compression set (%)	D395	25	32	Automatic transmission fluid	125	33
168 h		100	49			
Brittle point (°C)	D746	–	−57			

[a] Tested for 166 h

Table 2 Some physical properties of solvents used as penetrants at 25°C

Alkane	η (mPa s)	ε	V ($cm^3\ mol^{-1}$)	δ ($cal^{1/2}\ cm^{-3/2}$)
n-Pentane	0.23[a]	1.84[a]	115.2	7.10
n-Hexane	0.29	1.88	131.6	7.27
n-Heptane	0.40	1.93	147.5	7.43
n-Octane	0.52	1.95	163.5	7.57
n-Nonane	0.67	1.97	179.7	7.65
n-Decane	0.86	1.99	195.9	7.72
n-Dodecane	1.38	2.00	228.6	7.84
n-Tetradecane	2.04	2.04	260.1	7.96
n-Hexadecane	3.01	2.09	292.8	8.01
2,2,4-Trimethylpentane	0.47	1.94	166.1	6.85
Cyclohexane	0.90	2.02[a]	108.8	8.20
1,2,3,4-Tetrahydronaphthalene	2.00	2.77	136.8	9.50

[a] Taken at 20°C

S–D–RS–RD experiments

Circular cut and dried Santoprene samples weighing initially (W_0) ~0.4630 g were placed in screw-tight test bottles containing 15–20 ml of the respective solvents. These were periodically removed, the surfaces were dried by filter paper and the samples were weighed (W_t) on a digital Mettler balance (model AE 240, Switzerland) to within an accuracy of ±0.01 mg. Samples reached equilibrium saturation within 24 h and this did not change significantly over a further period of 1 or 2 days. The percentage weight gain during solvent sorption was calculated as:

$$\text{Wt}\%\,(t)=\left(\frac{W_t-W_0}{W_0}\right)\times 100 \qquad (1)$$

After completion of sorption experiments, the samples were placed in a vacuum for desorption measurements. The decrease in weight was monitored periodically. The total weight loss after desorption was calculated as:

$$\text{Wt loss }\%=\left(\frac{W_0-W_d}{W_0}\right)\times 100 \qquad (2)$$

where W_d is the weight of the Santoprene after desorption.

Resorption testing was carried out in the same way as the sorption tests. If the polymer does not show a weight loss during sorption and desorption, the initial weight of Santoprene and weight after desorption should be the same. In the present study, weight loss of Santoprene occurred in sorption and resorption experiments. The resorbed samples were placed once again in a vacuum for a second desorption. Any difference between the weight loss after redesorption indicates a continued weight loss during resorption. This is another way of testing the extent of continuous loss during S–D–RS–RD testing. The results confirm the agreement of the equilibrium sorption value M_∞, during desorption and redesorption. The observed total losses in S–D–RS–RD experiments are listed in *Table 3*. The mol% mass change (i.e. moles of solvent sorbed or desorbed per 100 g of polymer) in resorption experiments is generally higher than those observed in sorption experiments indicating higher saturation. However, in desorption and redesorption experiments, the mol% mass change remains almost identical.

RESULTS AND DISCUSSION

Sorption behaviour

The results of dynamic penetrant transport into a network polymer give a better understanding of the mechanisms of solvent transport. Earlier, we have investigated the mechanisms of alkane transport into several rubbery polymers[12,13]. Continuing these approaches, the penetrant sorption has been analysed in terms of the empirical relation[24,25]:

$$\log\left(\frac{M_t}{M_\infty}\right)=\log K+n\log t \qquad (3)$$

where M_t is the mass of solvent sorbed at time t, M_∞ is the mass of solvent sorbed at complete equilibrium and K is a parameter which depends on the structural characteristics of the polymer in addition to its interaction with solvent molecules. The value of n is indicative of the type of transport mechanism. In desorption, M_t and M_∞ represent, respectively, the mass loss of the drying samples at time t and the completely dried samples. Equation (3) is applicable for a preliminary analysis of sorption data up to 55% of the final weight of the solvent sorbed and it has no provisions for analysis of such details as inflections or solvent loss with time. The estimated values of n and K for sorption and resorption are compiled in *Table 4*. The values of n are accurate to ±0.01 units.

The values of n for sorption experiments vary between 0.50 and 0.62 in the investigated temperature range suggesting that the observed diffusion mechanism appears to follow Fickian-type transport. For the resorption process at 25°C, the values of n range from 0.54 to 0.59. However, the values of K tend to increase with a rise in temperature but decrease systematically with an increase in the molecular size of alkanes from n-heptane to n-hexadecane suggesting decreased polymer–solvent

Table 3 Mole per cent mass change and total weight loss during S–D–RS–RD experiments at 25°C

Alkane	Mass change (mol%)				Total mass loss (%) after	
	S	D	RS	RD	S–D cycle	RS–RD cycle
n-Pentane	0.096	0.424	0.564	0.428	26.1	1.75
n-Hexane	0.138	0.386	0.523	0.352	25.5	0.55
n-Heptane	0.142	0.346	0.503	0.330	26.6	−0.67
n-Octane	0.164	0.321	0.486	0.305	25.2	−0.12
n-Nonane	0.122	0.275	0.402	0.257	26.4	−1.47
n-Decane	0.111	0.249	0.346	0.237	25.2	1.15
n-Dodecane	0.088	–	–	–	25.7	–
n-Tetradecane	0.079	–	–	–	24.0	–
n-Hexadecane	0.079	–	–	–	[a]	–
2,2,4-Trimethylpentane	0.091	0.280	0.393	0.261	26.3	−1.57
Cyclohexane	0.451	0.532	1.981	0.546	24.2	1.67
1,2,3,4-Tetrahydronaphthalene	0.253	0.337	0.537	0.288	26.0	[a]

[a] Reliable data not obtained

Table 4 Fitting parameters of equation (3) for Santoprene and alkanes

	n		10^2K ($g\,g^{-1}\,min^n$)	
	S	RS	S	RS
	25–70°C	25°C	25–70°C	25°C
n-Pentane	0.54	(0.56)	26.4	(6.5)
n-Hexane	0.54–0.57	(0.57)	15.1–20.5	(5.0)
n-Heptane	0.52–0.62	(0.59)	17.1–21.7	(3.8)
n-Octane	0.51–0.52	(0.57)	12.4–16.7	(4.0)
n-Nonane	0.51–0.57	(0.55)	12.2–18.7	(3.1)
n-Decane	0.52–0.53	(0.58)	11.0–15.3	(3.1)
n-Dodecane	0.51–0.54	(–[a])	7.8–12.2	(–[a])
n-Tetradecane	0.50–0.53	(–[a])	6.2–10.4	(–[a])
n-Hexadecane	0.50–0.52	(–[a])	4.6–10.2	(–[a])
2,2,4-Trimethylpentane	0.52–0.56	(0.56)	10.3–15.2	(2.3)
Cyclohexane	0.57–0.61	(0.58)	6.2–9.0	(3.1)
1,2,3,4-Tetrahydronaphthalene	0.50–0.59	(0.54)	6.3–9.3	(2.0)

[a] Data not obtained due to high boiling points

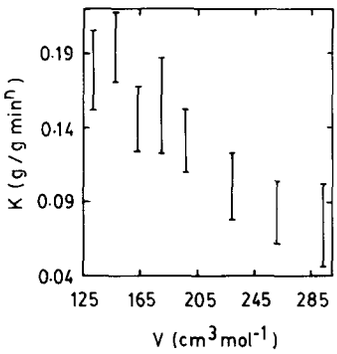

Figure 1 Dependence of parameter K of equation (3) on molar volume of n-alkanes. Vertical bars indicate the temperature interval of 25–70°C

interactions. The values of K for cyclohexane are almost identical to those of 1,2,3,4-tetrahydronaphthalene. The K values for 2,2,4-trimethylpentane are smaller than for n-octane for both sorption and resorption processes. On the other hand, the values of K for n-pentane and n-hexane do not follow the regular trend. The dependence of K on molar volume of alkanes in the investigated temperature interval is shown in *Figure 1*. For resorption, the values of K are smaller than those observed for sorption, possibly due to morphological changes of the polymer.

Data from sorption and desorption runs are presented as plots of the fractional uptake of the penetrant against $t^{1/2}/h$. These plots are referred to as reduced sorption/desorption curves, since the sheet thickness is included in the abscissa. This type of presentation is useful because it clearly shows any possible deviations of the penetrant transport from Fickian behaviour. Reduced plots of S–D–RS–RD experiments for lower n-alkanes, i.e. C_5 to C_{10} including 2,2,4-trimethylpentane (C_8) at 25°C are presented in *Figure 2*. For all penetrants, sorption uptake curves initially exhibited an overshoot effect with sudden maxima which later declined back to the true equilibrium values. Such overshoot effects have been attributed to changes in polymer morphology due to the presence of solvent molecules[19,26]. The observed overshoots in the present systems may be the result of morphological changes either from solvent-induced crystallization or from the possible phase separation occurring due to miscible blend morphology of Santoprene, thereby altering the conventional sorption phenomenon. The overshoot effect is not observed for desorption, resorption and redesorption processes as shown in *Figure 2*.

The observed overshoot effect for the sorption processes has been analysed by calculating the percentage overshoot index, OI[19]:

$$OI = \frac{M_m - M_\infty}{M_\infty} \times 100 \qquad (4)$$

where M_m is the maximum penetrant equilibrium. The values of OI at different temperatures are given in *Table 5* and these values at 25°C show a decrease with increasing size of alkanes except for n-octane. Among the penetrants studied, the OI at 25°C for n-pentane is highest (135). The OI results are not systematically dependent on temperature. The OI for 2,2,4-trimethylpentane is higher than for n-octane but for 2,2,4-trimethylpentane it decreases with an increase in temperature. At higher

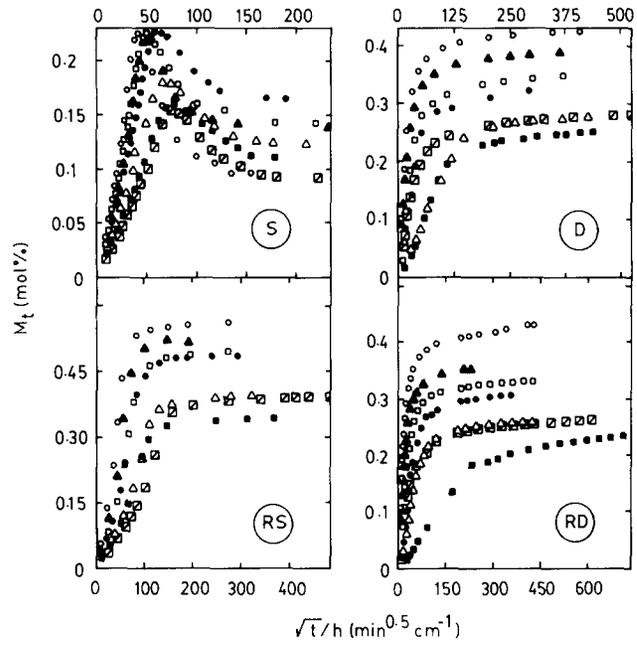

Figure 2 Reduced plots of mol% sorption, desorption, resorption, and redesorption at 25°C for (○) n-pentane, (▲) n-hexane, (□) n-heptane, (●) n-octane, (△) n-nonane, (■) n-decane and (▨) 2,2,4-trimethylpentane

Table 5 Per cent overshoot index values for Santoprene and alkanes at different temperatures

Alkanes	25°C	40°C	55°C	70°C
n-Pentane	135.4	–[a]	–[a]	–[a]
n-Hexane	63.2	61.5	53.4	–[a]
n-Heptane	57.3	69.5	52.9	42.6
n-Octane	37.9	36.9	30.4	23.6
n-Nonane	46.5	41.0	46.3	37.8
n-Decane	44.2	47.2	39.2	34.8
n-Dodecane	42.1	42.0	16.0	28.5
n-Tetradecane	33.1	48.0	32.3	20.8
n-Hexadecane	17.7	26.0	20.7	26.4
2,2,4-Trimethylpentane	68.1	58.9	55.6	45.6
Cyclohexane	11.9	10.7	8.8	2.0
1,2,3,4-Tetrahydronaphthalene	16.9	15.7	12.8	5.4

[a] Data not obtained due to low boiling points

temperatures, the *OI* values are generally smaller than at lower temperatures. The observed lower *OI* values for a bigger penetrant like n-hexadecane are attributed to the slow relaxation of the polymer chain in the presence of n-pentane.

Due to the observed overshoot effect in the present experimental systems, the sorption data have been analysed by shifting each of the fractional uptake curves based on the magnitude of the overshoot effect apparent in the plots (*Figure 2*). The shifting of the sorption curves can be expressed as[26]:

$$\frac{M_t}{M_\infty} - \alpha = Kt^n \qquad (5)$$

where α is a shift factor indicating the initial overshoot effect during sorption. The values of α, K and n have been determined at 95% confidence limit by fitting the experimental sorption results to equation (5) using the Marquardt's least squares procedure. The values of K and n as estimated from equation (5) for all the systems are almost identical to those given in *Table 4*.

In a sorption–desorption cycle, the available free volume of the polymer might increase and hence, the subsequent sorption process is different from that of the original. These effects have been successfully described by the network relaxation in terms of the times required for the molecular rearrangements of the chains and that of the solvent diffusion into the polymer[27]. However, segmental mobility of the polymer might be increased due to solvent ingression and this depends upon the ability of the solvent molecules to penetrate and, thereby, weaken the intermolecular forces of the polymer network structure.

The resorption curves for 2,2,4-trimethylpentane and n-nonane are almost identical at 25°C (*Figure 2*). Similarly, for n-heptane and n-pentane, the sorption curves are almost identical. Sorption curves for higher alkanes presented in *Figure 3* also exhibit significant overshoot effects for cyclohexane, n-dodecane and n-tetradecane; however, these effects are small for n-hexadecane and 1,2,3,4-tetrahydronaphthalene. Also, the equilibrium sorption values for n-hexadecane are lower than cyclohexane and other n-alkanes. The desorption curves for C_5 to C_{10} and 2,2,4-trimethylpentane presented in *Figure 2*, exhibit an increase in mol% desorption from alkanes C_5 to C_{10}. However, the desorption curves for n-decane are slightly sigmoidal; the desorption curves for 2,2,4-trimethylpentane and n-nonane are almost identical. The

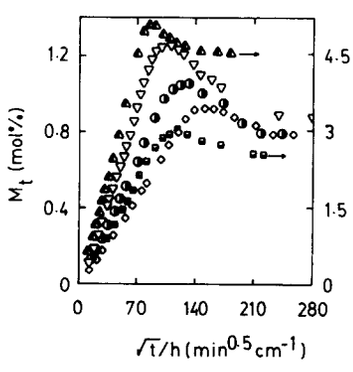

Figure 3 Reduced plots of mol% sorption at 25°C for (▽) n-dodecane, (◇) n-tetradecane, (◑) n-hexadecane, (▲) cyclohexane and (▬) 1,2,3,4-tetrahydronaphthalene

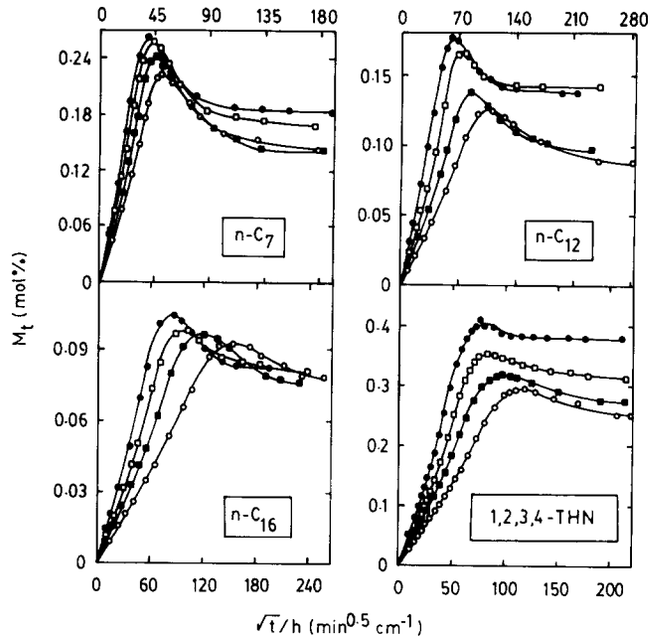

Figure 4 Effect of temperature on S–D–RS–RD curves for n-heptane, n-dodecane, n-hexadecane, and 1,2,3,4-tetrahydronaphthalene. Temperature: (○) 25°C; (■) 40°C; (□) 55°C; (●) 70°C

desorption experiments for high boiling alkanes (C_{12}, C_{14} and C_{16}) are not performed due to the difficulties in completely drying the Santoprene samples. The desorption and redesorption curves exhibit almost identical patterns. However, the equilibrium uptake values and the time to attain the equilibrium desorption are higher in redesorption than desorption. A striking difference is observed for n-decane which exhibits a more sigmoidal tendency in the redesorption process when compared to desorption. Also, the equilibrium desorption values for n-nonane and 2,2,4-trimethylpentane are almost identical. The behaviour of 2,2,4-trimethylpentane is quite different in S–D–RS–RD experiments, i.e. it exhibits lower sorption than all other penetrants presented in *Figure 2*. However, in desorption experiments, its value is higher than that of n-decane.

The temperature-dependent sorption curves for some representative penetrants, namely, n-heptane, n-dodecane, n-hexadecane and 1,2,3,4-tetrahydronaphthalene are given in *Figure 4*. For the latter, sorption increases with temperature and the overshoot effects are observed even at higher temperatures, but the effect is not systematic. It may be noted that the final equilibrium values for n-hexadecane lie within a narrow range of equilibrium sorption values. On the other hand, for n-heptane and n-dodecane, the values vary over a wider range. A plausible explanation for such an effect is that at high penetrant concentration during the later stages of sorption, the distribution of solvent molecules into the dense region of the polymer becomes significant. Also, at this stage a significant change in the network polymer structure might occur in the presence of some solvents.

The mol% sorption coefficients, S, obtained from the true equilibrium values for sorption and resorption processes in the investigated temperature interval are summarized in *Table 6*. Generally at 25°C, the mol% uptake data for sorption are considerably smaller than resorption. Sorption data at 25°C increase from n-pentane to n-octane and later show a decreasing tendency

Table 6 Sorption coefficients (S, mol%) for Santoprene and alkanes at different temperatures obtained from sorption and resorption runs

	Temperature (°C)				
	25		40	55	70
Alkanes	S	RS	S		
n-Pentane	0.096	(0.564)	–[a]	–[a]	–[a]
n-Hexane	0.138	(0.523)	0.151	0.180	–[a]
n-Heptane	0.142	(0.503)	0.143	0.169	0.184
n-Octane	0.164	(0.486)	0.186	0.210	0.232
n-Nonane	0.122	(0.402)	0.139	0.153	0.162
n-Decane	0.111	(0.346)	0.117	0.145	0.158
n-Dodecane	0.088	(–[b])	0.098	0.142	0.137
n-Tetradecane	0.079	(–[b])	0.074	0.093	0.110
n-Hexadecane	0.079	(–[b])	0.077	0;081	0.082
2,2,4-Trimethylpentane	0.081	(0.393)	0.105	0.117	0.131
Cyclohexane	0.451	(0.981)	0.519	0.610	0.723
1,2,3,4-Tetrahydronaphthalene	0.253	(0.537)	0.275	0.313	0.381

[a] Data not obtained due to low boiling points
[b] Data not obtained due to high boiling points

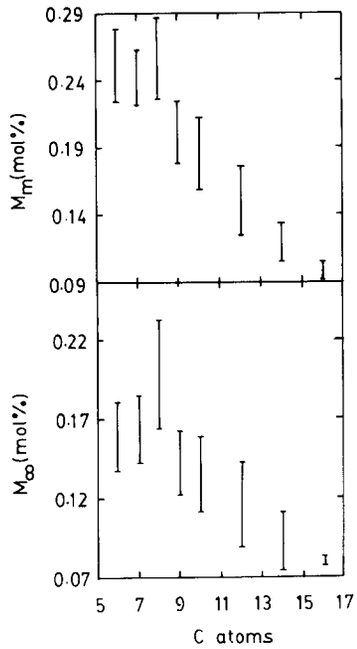

Figure 5 Dependence of maximum (M_m) and equilibrium (M_∞) sorption values on the number of carbon atoms of n-alkanes. Vertical bars indicate the temperature interval of 25–70°C

from n-nonane to n-hexadecane; for the latter penetrants, the S values are almost identical. The values of S for 2,2,4-trimethylpentane are smaller than for n-octane. A longer and bigger n-hexadecane exhibits an equilibrium sorption of 0.079 mol% at 25°C when compared to a value of 0.096 mol% for n-pentane. At higher temperatures, the values of S are not so systematic. It is interesting to note that the equilibrium resorption values at 25°C show a systematic decrease with an increase in the size of the alkanes from n-pentane to n-decane. The dependence of the maximum and equilibrium sorption values on the size of the n-alkanes (i.e. in terms of the number of carbon atoms) is given in *Figure 5*. It is noticed that except for n-octane, the remaining n-alkanes exhibit a decrease with increasing size of n-alkanes. From sorption results given in *Table 6*, it is obvious that though 2,2,4-trimethylpentane has the same number of carbon atoms as n-octane, its sorption is not identical; the sorption of the latter is higher. Also, the cyclic penetrants such as cyclohexane and 1,2,3,4-tetrahydronaphthalene exhibit higher sorption than the other n-alkanes.

There is a systematic increase in sorption with an increase in temperature except in a few cases. The sorption values of n-pentane at higher temperatures and n-hexane at 70°C are not available due to their low boiling points. Various parameters are critical in the interpretation of sorption results; these include temperature, penetrant size and shape, polarity and sample history. For instance, an increase in temperature should normally increase sorption; this is due to the creation of extra free volume. Within the investigated temperature range, the dynamic penetrant sorption tends to increase with temperature for all penetrants. The times to reach equilibrium (T_{eqm}) and maximum (T_{max}) sorptions also play an important role. This dependence is shown in *Figure 6*. Different T_{eqm} and T_{max} values are observed depending on the length of the penetrant molecules. Generally, T_{eqm} and T_{max} increase with increasing size of penetrants.

Calculation of diffusion coefficient

To calculate the overall average diffusion coefficient, D, of the penetrant into the polymer, Fick's second law of diffusion is solved for the slab geometry of the polymer immersed in an infinite solvent bath using the relation[28]:

$$\frac{M_t}{M_\infty} = 1 - \left(\frac{8}{\pi^2}\right) \sum_{n=0}^{\infty} \left\{ \left[\frac{1}{(2n+1)^2} \right] \exp\left[\frac{-D(2n+1)^2 \pi^2 t}{h^2} \right] \right\} \tag{6}$$

Equation (6) suggests that a plot of fractional equilibrium uptake *versus* $t^{1/2}/h$ is linear at small times so that D can be calculated from the initial slope. Sorption and desorption data were fitted to the first 11 terms of equation (6) (i.e. $n = 10$) using the Marquardt algorithm. At longer sorption times, equation (6) can be simplified to give:

$$\ln(1 - M_t/M_\infty) = \ln\left(\frac{8}{\pi^2}\right) - \frac{D\pi^2 t}{h^2} \tag{7}$$

Thus, a plot of $\ln(1 - M_t/M_\infty)$ *versus* t should be linear at long diffusion times and the slope is directly proportional to D. Some of our data presented in *Figure 7* show linearity only up to ~50% sorption equilibrium and

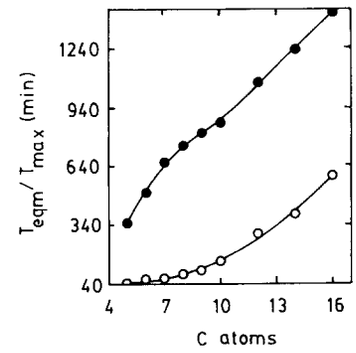

Figure 6 Dependence of maximum (○, T_{max}) and equilibrium (●, T_{eqm}) times on the number of carbon atoms of n-alkanes at 25°C

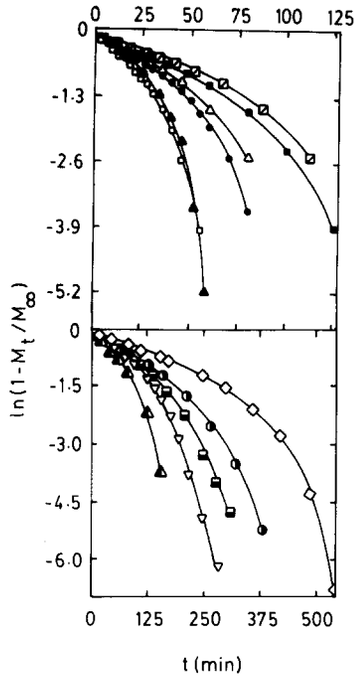

Figure 7 Long-term sorption plots according to equation (7) for Santoprene and n-alkanes at 25°C. Symbols are the same as in *Figures 2* and *3*

Table 7 Diffusion (D) and permeation (P) coefficients of Santoprene and alkanes from sorption measurements at different temperatures

	Temperature (°C)			
Alkanes	25	40	55	70
		$10^6 D$ (cm^2 s^{-1})		
n-Pentane	6.73	–[a]	–[a]	–[a]
n-Hexane	2.44	3.84	4.57	–[a]
n-Heptane	3.03	4.48	4.68	4.63
n-Octane	1.57	2.07	2.17	2.60
n-Nonane	1.61	1.87	2.84	3.69
n-Decane	1.24	1.67	1.92	2.44
n-Dodecane	0.65	0.96	0.88	1.70
n-Tetradecane	0.42	0.55	0.96	1.07
n-Hexadecane	0.22	0.45	0.61	0.95
2,2,4-Trimethylpentane	1.26	1.58	1.95	2.35
Cyclohexane	0.55	0.80	1.01	1.17
1,2,3,4-Tetrahydronaphthalene	0.40	0.61	0.62	0.80
		$10^7 P$ (cm^2 s^{-1})		
n-Pentane	4.64	–[a]	–[a]	–[a]
n-Hexane	2.89	5.00	7.11	–[a]
n-Heptane	4.30	6.40	7.93	8.51
n-Octane	2.94	4.39	5.21	6.87
n-Nonane	2.52	3.34	5.57	7.67
n-Decane	1.95	2.77	3.95	5.48
n-Dodecane	0.97	1.59	2.13	3.97
n-Tetradecane	0.67	0.81	1.77	2.34
n-Hexadecane	0.40	0.77	1.12	1.77
2,2,4-Trimethylpentane	1.32	1.90	2.60	3.51
Cyclohexane	2.07	3.51	5.20	7.10
1,2,3,4-Tetrahydronaphthalene	1.35	2.20	2.55	4.03

[a] Data not obtained due to low boiling points

slopes were calculated from these lines using least squares procedures. The diffusion coefficients obtained using equation (7) are somewhat higher than the D values calculated from equation (6). However, we used the D values calculated from equation (6) for our discussion. These values are compiled in *Table 7*.

The decrease of D from n-pentane to n-hexane is considerable when compared to the values from n-hexane to n-hexadecane. However, a systematic decrease in D is observed (with a few exceptions) at all the temperatures suggesting the dependence of D on the molecular size of the penetrant. A plot of D *versus* the number of carbon atoms showing this effect is shown in *Figure 8*. Earlier, it was realized[29,30] that the shape of the penetrant has a systematic effect on its transport into polymers. A linear and flexible molecule is expected to diffuse faster than a somewhat less flexible and less symmetrical molecule such as 2,2,4-trimethylpentane, cyclohexane and 1,2,3,4-tetrahydronaphthalene. In the present work, it was found that at all temperatures studied, the values of D for 2,2,4-trimethylpentane are lower than the values of a linear molecule of the same size (n-octane). This is because the pendent methyl groups in 2,2,4-trimethylpentane with its larger diameter may not locate an appropriate hole size in the polymer matrix.

Diffusion of a number of homologous paraffin hydrocarbons has been studied by Aitken and Barrer[31]. They found that the side methyl groups in the penetrants lowered the diffusivities more than in the case of the corresponding linear molecules. Conversely, when penetrant molecules are of comparable diameter but of varying length, the effect of the length of the molecule will play a dominant role. This was the case for the flexible and long chain molecule such as n-hexadecane, whose diffusion coefficients are smaller than other lower n-alkanes. The diffusion coefficients of cyclohexane are higher than 1,2,3,4-tetrahydronaphthalene at all the temperatures.

Diffusion in rubbery polymers bears a direct relationship to some of the solvent properties such as viscosity (η) and dielectric constant (ε). Vahdat[32], in a recent study, suggested a correlation between diffusivity and viscosity for elastomer–solvent systems. Similarly, for the present systems, a systematic variation of η and ε is observed with diffusion coefficients (*Figure 9*). Solvent permeation through a polymer film involves a macroscopic process, which results from the combination of two quite different local mechanisms[11–18]: the solubility of the solvent (in g g^{-1}) and the diffusion of the solvent, which is an irreversible kinetic process[28]. More simply, permeability, P, can be calculated as the product of the diffusion coefficient and solubility of the liquid in the membrane, i.e. $P = DS$. These results are also included in *Table 7*. It is generally observed that permeability results follow the same pattern as those of diffusion coefficients in the

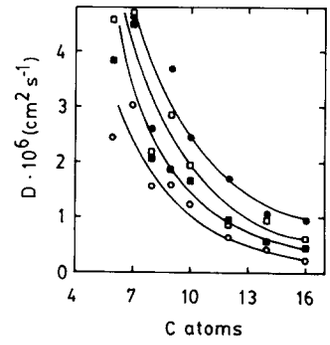

Figure 8 Dependence of diffusion coefficient on number of carbon atoms of n-alkanes at the temperatures given in *Figure 4*

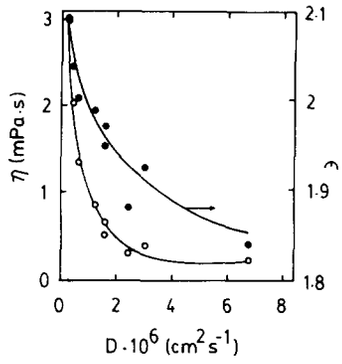

Figure 9 Dependence of (○) viscosity and (●) dielectric constant on the diffusion coefficient for Santoprene and n-alkanes at 25°C

Table 8 Comparison of diffusion and permeation coefficients from S–D–RS–RD experiments at 25°C for Santoprene and alkanes

Alkanes	S	D	RS	RD
		$10^6 D$ (cm^2 s^{-1})		
n-Pentane	6.73	2.32	0.41	0.24
n-Hexane	2.44	2.07	0.29	1.75
n-Heptane	3.03	0.69	0.20	0.64
n-Octane	1.57	0.54	0.20	0.23
n-Nonane	1.61	0.09	0.11	0.20
n-Decane	1.24	0.06	0.12	0.01
2,2,4-Trimethylpentane	1.26	0.61	0.06	0.47
Cyclohexane	0.55	0.92	0.14	0.65
1,2,3,4-Tetrahydronaphthalene	0.40	0.01	0.04	–[a]
		$10^7 P$ (cm^2 s^{-1})		
n-Pentane	4.64	7.09	1.67	7.53
n-Hexane	2.89	6.89	1.32	5.30
n-Heptane	4.30	2.40	1.00	2.11
n-Octane	2.94	1.99	1.13	0.79
n-Nonane	2.52	0.32	0.58	0.64
n-Decane	1.95	0.21	0.60	0.05
2,2,4-Trimethylpentane	1.32	1.95	0.28	1.41
Cyclohexane	2.07	4.12	1.16	2.98
1,2,3,4-Tetrahydronaphthalene	1.35	0.05	0.31	–[a]

[a] Reliable data not obtained

investigated temperature range. Permeability results of cyclohexane are higher than 1,2,3,4-tetrahydronaphthalene. Permeability of n-octane is higher than that of 2,2,4-trimethylpentane. A comparison of diffusion and permeation coefficients at 25°C for the S–D–RS–RD experiments is given in *Table 8*. The values of these coefficients are different in all these processes suggesting possible morphological changes of Santoprene in the presence of different molecules during the cyclic S–D–RS–RD testing. Similarly, the diffusion and permeation coefficients for 1,2,3,4-tetrahydronaphthalene are quite small.

Sorption kinetics

Earlier, it was shown that sorption in rubbery polymers can be studied by using first-order kinetics[33]. Continuing this approach, we have calculated the first-order rate constant k_1, by using the following equation:

$$dM/dt = k_1(M_\infty - M_t) \quad (8)$$

which upon integration gives

$$k_1 t = \ln [M_\infty/(M_\infty - M_t)] \quad (9)$$

A representative first-order plot of $\log(M_\infty - M_t)$ *versus* t is shown in *Figure 10*. For all solvents these plots exhibit negative slopes and are slightly curved. The calculated values of the rate constants in the temperature interval 25–70°C are given in *Table 9*. The k_1 values follow a regular trend of increasing with temperature and show

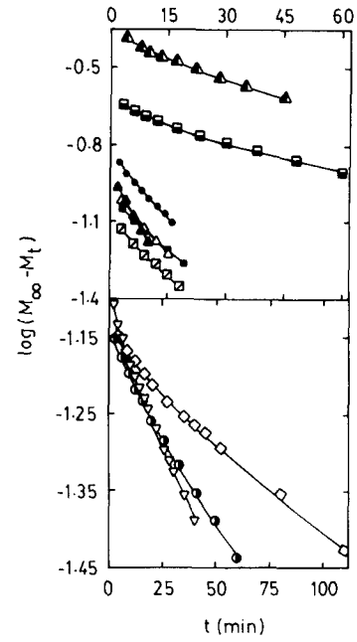

Figure 10 First-order kinetics plots for Santoprene and n-alkanes at 25°C. Symbols are the same as in *Figures 2* and *3*

Table 9 First- (k_1) and second-order (k_2) rate constants for Santoprene and alkanes at different temperatures obtained from sorption and resorption runs

	Temperature (°C)				
	25		40	55	70
Alkanes	S	R	S		
		$10^2 k_1$ (min^{-1})			
n-Pentane	–[a]	(1.78)	–[b]	–[b]	–[b]
n-Hexane	6.25	(1.20)	9.82	11.78	–[b]
n-Heptane	7.00	(0.84)	9.88	11.04	12.96
n-Octane	3.74	(0.82)	5.03	6.34	6.26
n-Nonane	3.94	(0.49)	5.00	6.66	8.92
n-Decane	3.04	(0.55)	4.06	4.59	5.71
n-Dodecane	1.67	(–[c])	2.29	2.17	4.07
n-Tetradecane	1.11	(–[c])	1.50	2.27	2.60
n-Hexadecane	0.61	(–[c])	1.08	1.49	2.27
2,2,4-Trimethylpentane	3.33	(0.29)	4.01	4.98	5.82
Cyclohexane	1.54	(0.61)	2.17	2.82	3.10
1,2,3,4-Tetrahydronaphthalene	1.03	(0.18)	1.48	1.75	1.96
		$10k_2$ (mol^{-1} min^{-1})			
n-Pentane	–[a]	(1.78)	–[b]	–[b]	–[b]
n-Hexane	18.86	(1.12)	27.55	26.30	–[b]
n-Heptane	18.85	(0.70)	27.32	22.88	24.66
n-Octane	6.92	(0.61)	8.41	9.10	8.65
n-Nonane	8.91	(0.39)	9.87	11.89	15.25
n-Decane	6.70	(0.44)	8.79	7.81	8.90
n-Dodecane	3.79	(–[c])	4.76	2.99	6.17
n-Tetradecane	2.41	(–[c])	3.44	4.28	4.01
n-Hexadecane	1.11	(–[c])	2.12	2.73	4.17
2,2,4-Trimethylpentane	11.04	(0.26)	11.74	12.29	13.72
Cyclohexane	1.36	(0.29)	1.69	1.85	1.77
1,2,3,4-Tetrahydronaphthalene	1.02	(0.10)	1.33	1.47	1.29

[a] Data not obtained due to quick sorption within 5 min
[b] Data not obtained due to low boiling points
[c] Data not obtained due to high boiling points

a decreasing trend from n-heptane to n-hexadecane. This is expected in view of the fact that the diffusivity values are proportional to the k_1 values as shown below.

For long sorption times, the term $n \geqslant 1$ as well as $\ln(8/\pi^2)$ can be ignored so that equation (6) simplifies to give:

$$\ln\left(\frac{M_\infty}{M_\infty - M_t}\right) \cong \frac{\pi^2 Dt}{h^2} \tag{10}$$

Equation (10) is identical to equation (9) when

$$k_1 = \frac{\pi^2 D}{h^2} \tag{11}$$

For extensive swelling, h^2 obviously does not remain constant and hence, D increases due to the influx of the solvent into the polymer matrix. If swelling becomes considerable, then it is legitimate to apply second-order kinetics using the following empirical equation[34]:

$$\frac{t}{Q} = A + Bt \tag{12}$$

where A and B are numerical constants. At long times, $Bt > A$ so that $B = 1/Q_\infty$. At short times, $A > Bt$ so that the quantity $1/A = \lim_{t \to 0}(dQ/dt)$ represents the initial rate of swelling, when the polymer network just begins to relax in response to the osmotic pressure. The equation for second-order swelling is then given as:

$$\frac{dM}{dt} = k_2(M_\infty - M_t)^2 \tag{13}$$

where k_2 is the second-order rate constant. The integrated form of the equation representing the swelling rate at time t is given by:

$$M_t = \frac{k_2 M_\infty^2 t}{1 + k_2 M_\infty t} \tag{14}$$

which upon further simplification gives

$$k_2 t = \frac{M_t}{M_\infty(M_\infty - M_t)} \quad \text{or} \quad k_2 t = \frac{1}{M_\infty - M_t} - \frac{1}{M_\infty} \tag{15}$$

where $k_2 = 1/AC_\infty^2$ (*Table 9*). Detailed explanations for the use of second-order swelling kinetics have been given earlier by Schott[34].

A typical second-order kinetics plot for n-alkanes at 25°C is given in *Figure 11* and supports the use of second-order kinetics for the systems in this study. However, the plot shows a slight curvature and the early portion is a straight line. From the slope of this curve, the values of k_2 have been obtained; these values are generally smaller than k_1 values for all the Santoprene and solvent systems. In view of the non-swelling tendencies of Santoprene samples for the solvents used in the present study, first-order kinetics seem to be more likely than second-order kinetics.

Temperature effects and activation parameters

Theoretical developments in the past decades have led to the understanding that for most of the rubbery polymers well above their glass transition temperatures, the Arrhenius relation is generally valid[35]; curved plots are also observed when larger temperature ranges are investigated[36]. We have analysed the diffusion results

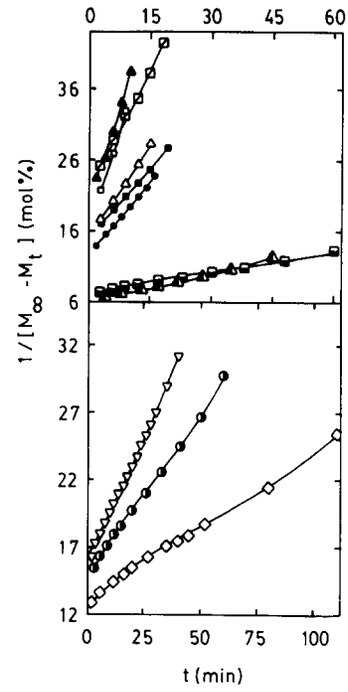

Figure 11 Second-order kinetics plots for Santoprene and n-alkanes at 25°C. Symbols are the same as in *Figures 2* and *3*

based on the Arrhenius relation for the diffusion process:

$$D = D_0 \exp(-E_D/RT) \tag{16}$$

where E_D is the activation energy of diffusion which is a function of the intra- and interchain forces which must be overcome in order to create the space for a unit diffusional jump of the penetrant molecule, D_0 is a pre-exponential factor and RT has its conventional meaning. The activation energy will be greater the larger the penetrant molecule, the stronger the polymer cohesive energy, and the more rigid the polymer chain segments. Similarly, the sorption coefficient S can be expressed in terms of the van't Hoff equation with a pre-exponential factor S_0:

$$S = S_0 \exp(-\Delta H_S/RT) \tag{17}$$

Here, ΔH_S is the heat of sorption which is a composite parameter involving contributions from Henry's law and Langmuir-type sorption.

Since the permeability coefficient P is a combination of diffusion and sorption processes the activation energy, E_P, for permeation is given as:

$$E_P = E_D + \Delta H_S \tag{18}$$

Equations (16) and (17) were used to calculate E_D and ΔH_S from the least-squares procedure.

Figure 12 displays the dependence of $\log D$ on $1/T$, wherein a slight non-linearity is observed in many cases over the investigated temperature range. The E_P values were calculated from equation (18) and these results are included in *Table 10*. Due to the slight non-linearity in the $\log D$ *versus* $1/T$ plots, the values of E_D or E_P do not seem to follow any regular trend with the penetrant size. The lowest values of E_D of ~ 7–$8\ \text{kJ mol}^{-1}$ are observed for n-heptane and n-octane while the highest value of $\sim 26\ \text{kJ mol}^{-1}$ is found for n-hexadecane. Activation parameters for 2,2,4-trimethylpentane are higher than for n-octane; similar data for 1,2,3,4-tetrahydronaphthalene

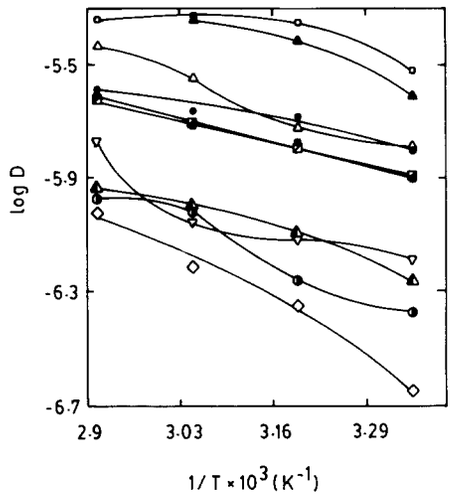

Figure 12 Arrhenius plots for the dependence of $\log D$ on $1/T$ for Santoprene and n-alkanes. Symbols are the same as in *Figures 2* and *3*

Table 10 Activation parameters (E_D, E_P and ΔH_S, all in kJ mol^{-1}), interaction parameter (χ) and molar mass between physical entanglement crosslinks ($\bar{M}_C$) for Santoprene and alkanes

Alkanes	E_D	E_P	ΔH_S	χ	$\bar{M}_C$
n-Pentane	–	–	–	0.383	50
n-Hexane	17.13	24.44	7.31	0.360	81
n-Heptane	7.67	13.00	5.33	0.345	102
n-Octane	8.89	15.45	6.57	0.340	141
n-Nonane	16.42	21.79	5.37	0.342	129
n-Decane	12.33	19.55	7.22	0.347	140
n-Dodecane	15.83	25.59	9.77	0.368	156
n-Tetradecane	18.95	25.70	6.75	0.407	189
n-Hexadecane	26.44	27.48	1.04	0.436	244
2,2,4-Trimethylpentane	11.78	18.45	6.67	0.485	99
Cyclohexane	14.35	23.27	8.92	0.413	205
1,2,3,4-Tetrahydronaphthalene	11.82	19.47	7.65	1.201	–[a]

[a] Negative value observed

are lower than for cyclohexane. However, an increase of ~ 3 kJ mol^{-1} in E_D or E_P values for the 2,2,4-trimethylpentane molecule is due to the presence of three pendent methyl groups requiring a larger hole size and thus exhibits a higher E_D than its equivalent isomer n-octane of almost the same size. It may be noted that for all the penetrants, the values of ΔH_S are positive suggesting that the sorption is mainly dominated by the Henry's law sorption mode giving an endothermic contribution to the sorption process.

Interaction parameter and molar mass between crosslinks

The equilibrium swelling experiments have been used to determine the molar mass between crosslinks $\bar{M}_C$ by the procedures suggested by Flory and Rehner[37]. Thus, for a perfect polymer network:

$$\bar{M}_C = \frac{-\rho_P V_S(\phi_P^{1/3} - \phi_P^{1/2})}{\ln(1-\phi_P) + \phi_P + \chi\phi_P^2} \quad (19)$$

where V_S is the molar volume of the solvent, ρ_p is the polymer density, ϕ_p is the volume fraction of the polymer in the swollen state. This is calculated as [38]:

$$\phi_P = \left[1 + \frac{\rho_P}{\rho_S}\left(\frac{M_a}{M_b}\right) - \frac{\rho_P}{\rho_S}\right]^{-1} \quad (20)$$

where M_b and M_a are, respectively, the mass of the polymer before and after swelling, ρ_S is solvent density and ρ_P is the density of Santoprene. The parameter χ has the conventional meaning from the Flory–Huggins theory of dilute polymer solutions.

From a refinement of the lattice model, Huggins[39] deduced that χ should be expressed approximately by:

$$\chi = \beta + \frac{V_S}{RT}(\delta_S - \delta_p)^2 \quad (21)$$

where δ_S is the solubility parameter of the solvent and β is a lattice constant whose value is generally taken to be 0.34 for elastomer–solvent systems. To calculate χ, the value of the solubility parameter of the polymer δ_p is needed. The procedure used by Gee[40] and Takahashi[41] is used for this purpose. A plot of the swelling coefficient $\alpha = (M_a - M_b)/M_b\rho_s$ *versus* δ_s is constructed. The maximum value in α is found at $\delta_S = 7.57$ and this gives δ_p. Using this value, χ is calculated from equation (21). The values of $\bar{M}_C$ are calculated using equation (19). These data are also included in *Table 10*.

The values of $\bar{M}_C$ show some general tendency to increase with the chain length of the n-alkanes. Because the nature of the crosslinked system is understood either in terms of $\bar{M}_C$ or in terms of its reciprocal value, which will be indicative of the crosslink density, it is evident that the crosslink density decreases with an increase in the size of the penetrant molecules; therefore, the values of $\bar{M}_C$ may be regarded as physical crosslink entanglements rather than chemical crosslinks. The values of $\bar{M}_C$ range from the lowest value of 50 for n-pentane to the highest value of 244 for n-hexadecane. For 1,2,3,4-tetrahydronaphthalene, we could not obtain reliable $\bar{M}_C$ data. The estimation of $\bar{M}_C$ using the Flory–Rehner theory has limited applications for the type of polymer–solvent systems studied here and hence, these values should be regarded as only approximate. However, the data presented here serve as a qualitatively successful application of the Flory–Rehner theory.

CONCLUSIONS

Sorption and transport characteristics of Santoprene in a variety of solvent media have been studied by the use of a sorption gravimetric technique. Such a study is important in applications including pervaporation, barrier packaging, controlled delivery of biologically active materials, plasticizer migration, physical ageing, etc. The results of the study on polymer–solvent interactions is important for successful applications of these materials in situations involving solvents. The transport coefficients of this study have shown a dependence on the penetrant size, concentration, temperature and morphology of Santoprene. The diffusivity values of 2,2,4-trimethylpentane at all temperatures were considerably lower than the corresponding values for a linear molecule of a similar size, namely n-octane. This is attributed to the rigidity of 2,2,4-trimethylpentane. Also, 2,2,4-trimethylpentane exhibits a higher value of E_D than n-octane. At higher temperature, the increase in diffusion and relaxation rates of the polymer, accompanied by the increase in the polymer free volume might have resulted in a higher equilibrium penetrant uptake. The observed overshoot

effect with the present systems was attributed to the complicated two-phase polymer morphology. However, more research is necessary.

Transport kinetics has been studied in terms of the first- and second-order kinetics model. However, it is difficult to characterize the overall transport kinetics with a specific experimental parameter. First-order kinetics seems to be more appropriate for the systems studied. The diffusion coefficients have been estimated from the Fickian equation. The morphological changes in Santoprene samples have been studied by estimating the molar mass between physical entanglement crosslinks. None of the solvents used has shown any degradative reactions towards Santoprene during the course of this study.

ACKNOWLEDGEMENT

We thank the Council of Scientific and Industrial Research (grant no. 01(1239)/92/EMR-II) for financial support.

REFERENCES

1 Kulkarni, P. V., Rajur, S. B., Antich, P., Aminabhavi, T. M. and Aralaguppi, M. I. *J. Macromol. Sci., Rev. Macromol. Chem. Phys.* 1990, **C30**, 441
2 Huang, R. Y. M. (Ed.) 'Pervaporation Membrane Separation Processes', Elsevier, New York, 1991
3 Aminabhavi, T. M., Harogoppad, S. B., Khinnavar, R. S. and Balundgi, R. H. *J. Macromol. Sci., Rev. Macromol. Chem. Phys.* 1991, **C31**(4), 433
4 Seymour, R. B. 'Engineering Polymer Source Book', McGraw Hill, New York, 1990
5 Khinnavar, R. S., Aminabhavi, T. M., Kutac, A. and Shukla, S. S. *J. Hazardous Mater.* 1991, **28**, 281
6 Cassidy, P. E., Mores, M., Kerwick, D. J., Koech, D. J., Verschoor, K. L. and White, D. F. *Geotextiles Geomembranes* 1992, **11**, 61
7 Fang, Y., Sourirajan, S. and Matsuura, T. *J. Appl. Polym. Sci.* 1992, **44**, 1959
8 Sourirajan, S. 'Reverse Osmosis', Academic Press, New York, 1970
9 Aminabhavi, T. M., Khinnavar, R. S., Harogoppad, S. B., Aithal, U. S., Nguyen, Q. T. and Hansen, K. C. *J. Macromol. Sci., Rev. Macromol. Chem. Phys.* 1994, **634**, 139
10 David, M. O., Nguyen, Q. T. and Neel, J. *J. Membr. Sci.* 1992, **73**, 129
11 Aminabhavi, T. M. and Munnolli, R. S. *Polym. Int.* 1994, **34**, 59
12 Harogoppad, S. B. and Aminabhavi, T. M. *Macromolecules* 1991, **24**, 2598
13 Khinnavar, R. S. and Aminabhavi, T. M. *J. Appl. Polym. Sci.* 1991, **42**, 2321
14 Aithal, U. S., Aminabhavi, T. M. and Cassidy, P. E. *J. Membr. Sci.* 1990, **50**, 225
15 Aminabhavi, T. M., Munnolli, R. S., Stahl, W. M. and Gangal, S. V. *J. Appl. Polym. Sci.* 1993, **48**, 857
16 Khinnavar, R. S. and Aminabhavi, T. M. *Polymer* 1993, **34**, 1006
17 Harogoppad, S. B. and Aminabhavi, T. M. *J. Appl. Polym. Sci.* 1992, **46**, 725
18 Harogoppad, S. B. and Aminabhavi, T. M. *Polymer* 1991, **32**, 870
19 Kim, D., Caruthers, J. M. and Peppas, N. A. *Macromolecules* 1993, **26**, 1841
20 Johnson, H. E., Clarson, S. J. and Granick, S. *Polymer* 1993, **34**, 1960
21 Peppas, N. A. and Urdahl, K. G. *Eur. Polym. J.* 1988, **24**, 13
22 Walker, C. M. and Peppas, N. A. *J. Appl. Polym. Sci.* 1990, **39**, 2043
23 Riddick, J. A. and Bunger, W. B. in 'Techniques in Chemistry', Vol. 2, 3rd Edn, Wiley-Interscience, New York, 1970
24 Urdahl, K. G. and Peppas, N. A. *J. Appl. Polym. Sci.* 1987, **33**, 2669
25 Urdahl, K. G. and Peppas, N. A. *Polym. Eng. Sci.* 1988, **28**, 96
26 Shieh, L. Y. and Peppas, N. A. *J. Appl. Polym. Sci.* 1991, **42**, 1579
27 Ferry, J. D. in 'Viscoelastic Properties of Polymers', John Wiley & Sons, New York, 1970
28 Crank, J. 'Mathematics of Diffusion', 2nd Edn, Clarendon, Oxford, 1975
29 Salem, M., Asfour, A. F. A., DeKee, D. and Harrison, B. *J. Appl. Polym. Sci.* 1989, **37**, 617
30 Brown, W. R., Jenkins, R. B. and Park, G. S. *J. Polym. Sci., Polym. Symp.* 1973, **41**, 45
31 Aitken, A. and Barrer, R. M. *Trans. Faraday Soc.* 1955, **51**, 116
32 Vahdat, N. *J. Appl. Polym. Sci.* 1991, **42**, 3165
33 Aminabhavi, T. M. and Harogoppad, S. B. *J. Chem. Educ.* 1991, **68**, 343
34 Schott, H. *J. Macromol. Sci. Phys.* 1992, **B31**, 1
35 Aminabhavi, T. M., Aithal, U. S. and Shukla, S. S. *J. Macromol. Sci. Chem. Phys.* 1988, **C28** (3 and 4), 421
36 Hayer, M. J. and Park, G. S. *Trans. Faraday Soc.* 1955, **51**, 1134
37 Flory, P. J. and Rehner Jr, J. *J. Chem. Phys.* 1943, **11**, 521
38 Aithal, U. S., Aminabhavi, T. M. and Cassidy, P. E. *Am. Chem. Soc. Symp. Ser.* 1990, **423**, 351
39 Huggins, M. L. *J. Chem. Phys.* 1941, **9**, 440
40 Gee, G. *Trans. Faraday Soc.* 1942, **38**, 418; 1944, **40**, 468
41 Takahashi, S. *J. Appl. Polym. Sci.* 1983, **28**, 2847